Signal Processing 135 (2017) 107–120

Contents lists available at ScienceDirect

Signal Processing

journal homepage: www.elsevier.com/locate/sigpro

A parametrization technique to design joint time–frequency optimized discrete-time biorthogonal wavelet bases

Manish Sharma[c,*], Achuth P. V.[b], Ram Bilas Pachori[a], Vikram M. Gadre[b]

[a] Discipline of Electrical Engineering, Indian Institute of Technology Indore, Indore 453552, India
[b] Department of Electrical Engineering, Indian Institute of Technology Bombay, Mumbai 400076, India
[c] Department of Electrical Engineering, Institute of Infrastructure, Technology, Research and Management (IITRAM), Ahmedabad, India

ARTICLE INFO

Keywords:
Biorthogonal wavelet bases
Parametrization
Joint time–frequency localization
Image coding

ABSTRACT

The accurate and efficient representation of a signal in terms of elementary atoms has been a challenge in many signal processing applications including harmonic analysis. The wavelet bases have been proved to be very efficient and flexible atoms. Towards the goal of obtaining optimal wavelet bases, we present a simple and efficient parametrization technique for constructing linear phase biorthogonal discrete-time wavelet bases that have joint time–frequency localization (JTFL) close to the lower bound of 0.25. In this paper, we first develop a parametrization technique to design biorthogonal filter banks (FBs). Then an optimization method is formulated to design jointly time–frequency localized discrete wavelet bases employing the designed FBs. Finally, the performance of the optimal wavelet bases is evaluated in image coding application. The proposed parametrization method presents a general and yet a very simple framework to construct a linear phase biorthogonal FB of desired order, with the prescribed number of vanishing moments (VMs) and free parameters. Several examples are presented to demonstrate the effectiveness and flexibility of the technique to design different classes of FB with various degrees of freedom. The performance of the designed FBs is compared with the other popular biorthogonal wavelet FBs.

1. Introduction

Decomposing a signal into its elementary atoms or bases is important in many signal processing applications and harmonic analysis. In the analysis of non-stationary signals, joint time–frequency localization (JTFL) of the bases is of paramount importance. However, the uncertainty principle poses a fundamental limit on the JTFL. It states that a signal cannot be arbitrarily localized in time and frequency simultaneously. Thus, the central challenge in harmonic and signal analysis is to obtain optimal bases, which are localized well in both time and frequency. Wavelet bases have very good JTFL and therefore have emerged as a powerful tool for signal analysis. Wavelet bases are extensively used in the analysis of non-stationary signals and have found applications in computer vision, transient and edge detection, medical imaging, pitch estimation, and image compression [1–3]. Besides, a variety of optimality criteria such as orthogonality, regularity, frequency selectivity, ripple energies in passband as well as in stopband and JTFL of the filters are considered to design optimal wavelet filter banks (WFBs) [4–7]. The selection of optimality criteria to design a FB depends on the application. The time–frequency localization of the filters is found playing the central role in many signal processing applications [8]. Therefore, in recent times, the WFBs have been designed considering JTFL as an optimality criterion [9–11]. The performance of JTFL optimized filters has been found to be excellent in image segmentation, image compression, feature extraction and edge detection by Wilson and Granlund [8]. In image coding applications, the performance of JTFL optimized orthogonal WFBs has been found to be better than other FBs by Monro et al. [12] and Morris et al. [13]. Recently, Dandach and Siohan [14] obtain that JTFL optimized WFBs perform well in reducing inter-symbol interference (ISI) and inter-channel interference in orthogonal frequency division multiplexing (OFDM) multi-carrier systems. Davidson et al. [15] demonstrate that the JTFL optimized WFBs are capable of reducing ISI in pulse shaping system. The performance of JTFL optimized WFBs has been found superior in compression and denoising of electrocardiogram (ECG) signals [7,16]. Thus, the JTFL is a pertinent criterion in designing WFBs.

There are mainly two techniques to design two-channel perfect reconstruction (PR) FBs: (i) factorization of Lagrange half band polynomial (LHBP) [17–20] and (ii) lattice structure and lifting

* Corresponding author.
E-mail addresses: manishsharma.iitb@gmail.com (M. Sharma), achuthpv@gmail.com (A.P. V.), pachori@iiti.ac.in (R.B. Pachori), vmgadre@ee.iitb.ac.in (V.M. Gadre).

http://dx.doi.org/10.1016/j.sigpro.2016.12.019
Received 13 September 2016; Received in revised form 12 December 2016; Accepted 17 December 2016
Available online 21 December 2016

scheme [21,22]. In factorization of LHBP, a half band product filter is first designed, and is then factored into the analysis and synthesis low-pass filters. Cohen et al. [19] have proposed a design method, for compactly supported biorthogonal WFBs, in which a LHBP which has the maximum number of zeros at, $z = -1$, is factorized to obtain analysis and synthesis low-pass filters. The LHBP is also known as a maximally flat filter. One of the limitations of this method is that we do not have any flexibility to control or optimize any attribute pertaining to the WFBs. Another disadvantage of this method is that the count of spectral factors grow linearly with respect to the degree of LHBP. Further, factorization of LHBP becomes increasingly difficult when the number of zeros at $z = -1$ increases. The FB design methods using lattice structures have been presented by Vaidyanathan and Hong [21] as well as by Vetterli and Herley [23]. In such structures, perfect reconstruction and linear phase properties are structurally imposed. But the vanishing moments (VMs) conditions are difficult to be incorporated in these structures as quantization of lattice parameters usually results in loss of VMs. Further, the number of lattice parameters grows linearly with the lengths of filters involved. The lifting scheme [22] requires fewer numerical computations than the lattice structure. However, VMs are almost lost due to quantization, similar to the lattice structures.

Therefore, a parametrization technique is highly desirable where both PR and VMs conditions can be imposed structurally, and the number of parameters remains fixed irrespective of the length of the filters. Aiming to achieve this objective, Tay [24] has presented a parametrization based technique to construct two-channel linear phase biorthogonal FBs. Herein, the author constructs families of 9/7 and 6/10 FBs, and derives their corresponding one-parameter and two-parameter expressions. Tay [24] also considered a family of 9/11 FBs with two free parameters; however, the explicit parametric expression for filters were not obtained. Though, the proposed parametrization technique presents an effective strategy to optimize the desired attributes of the FB, the parametrization technique is not general and is restrictive. The author considers the design of a family of a few FBs (9/7 and 6/10) with at the most two degrees of freedom only. In this paper, we propose a quite general framework to design parametrized biorthogonal FBs. The main differences between the proposed method and the method of Tay [24] are as follows: (i) The proposed parametrization technique is quite general and non-restrictive unlike the techniques presented by Tay [24]. The proposed method presents a simple framework for constructing a parametric FB of any order with the prescribed number of VMs and free parameters. Tay designs families of only lower order FBs, viz. 9/7 and 6/10, with at the most two free parameters, whereas we design relatively higher order FBs such as 9/15, 10/14, 8/16, 9/13, 13/11, 9/11, 10/10, 7/13, 8/12, 6/14, 5/15, 4/16 with the desired degrees of freedom (with one, two, three, four and more). The increased number of freedoms provides greater flexibility and control in the optimization. (ii) The prime objective of Tay [24] was to obtain filters with rational coefficients, whereas our aim is to obtain time–frequency localized discrete biorthogonal wavelet bases. Recently, Murugesan and Tay [25] have extended the work of Tay [24] to design higher order FBs employing the same philosophy of [24], by reducing the number of VMs. However, there are certain differences between the method proposed by us and that of [25]. The method of Murugesan and Tay [25] is restrictive. The fundamental restriction is that one cannot reduce VMs of both analysis as well as synthesis low-pass filters, simultaneously. The reduction on both filters leads to a system of non-linear equations. The solution of the set of nonlinear equations is not only difficult but also gives multiple and irrational solutions. However, in our proposed method it is possible to relax VMs on both filters simultaneously and still, need to solve a set of linear equations only. The equations yield a unique solution. Thus our method is more general and has lesser restrictions than the method of Murugesan and Tay [25] and thus applicable to design of any arbitrary biorthogonal pair of filters. Further, the aim of authors in [25] is to design FBs with rational coefficients whereas we intend to construct optimal JTFL wavelet bases.

Parhizkar et al. [26] design JTFL optimized windows employing circular spreads, proposed by Breitenberger [27]. Recently, Starosielec and Hagele [28] design JTFL optimized windows using variance based spreads. However, authors [26,28] do not consider the design of a FB. Tazebay and Akansu [29] design progressively time–frequency optimized subband tree structured orthogonal FBs. Tay et al. [7] design optimal root mean squared (RMS) bandwidth orthogonal filters. Morris and his collaborators [16,30,31] design JTFL localized orthogonal wavelets by optimizing lattice parameters. In the above approaches, authors consider the design of optimal orthogonal FBs without addressing the design of optimal biorthogonal WFBs. Although, orthogonal FBs satisfy the energy preservation property, they cannot simultaneously have linear phase property which is highly desirable in image coding applications. The linear phase property enables us to use symmetric extension methods which facilitate us to handle boundaries of compactly supported signals. The linear phase property also leads to faster and efficient implementation of FBs. Sharma et al. [10,11,32] present a class of JTFL optimized linear phase biorthogonal WFBs where the optimally time–frequency localized analysis low-pass filter (ALF) and synthesis low-pass filter (SLF) have been designed using an eigenfilter based technique. Similarly, Tay [33] also designs a special class of optimal biorthogonal FBs called half band pair FBs employing Bernestein polynomials where ALF and SLF are optimized for their JTFL. It is to be noted that iterations of the optimal ALF and SLF do not yield optimal discrete wavelet bases. Sharma et al. [34] also design a class of optimal biorthogonal WFBs in which they minimize the JTFL of the wavelet functions in $L_2(\mathbb{R})$ instead of ALF and SLF in $l_2(\mathbb{Z})$. However, the optimization of a wavelet function alone does not ensure the localization of all other bases employed in the multilevel decomposition of a signal.

In this paper, in order to exploit advantages of both the linear phase and JTFL properties, we propose a method to design time–frequency localized compactly supported linear phase biorthogonal WFBs. Here, the optimality criterion considers the JTFL of all basis sequences (which are obtained from iterations of the filters of the underlying FB) of the analysis and synthesis discrete-time wavelet bases. For the given J number of decomposition levels, the number of basis sequences corresponding to the wavelet basis is $J + 1$. To obtain optimal wavelet bases, we first design parametrized linear phase PR two-channel FBs with the prescribed VMs (regularity), lengths and degrees of freedom. This is followed by the optimization of independent (free) parameters to obtain FBs that yield optimal time–frequency localized discrete wavelet bases in $l_2(\mathbb{Z})$. Finally, the performance of the designed wavelet bases has been evaluated in image compression application.

The proposed parametrization technique is based on the following simple idea: some VMs (zeros at $z = -1$) of the LHBP are freed (relaxed) to obtain free parameters. This is followed by obtaining a system of linear equations which is derived from the half band condition on the product filter. The solution of the set of equations yields parametric expressions for filter coefficients. The entire proposed work can be summarized as follows: (i) First, we fix the number of free parameters, VMs and lengths of analysis and synthesis filters. (ii) Secondly, the ALF is defined as a symmetric polynomial in z. The polynomial can be expressed as the product of two factors. One factor is the binomial polynomial whose all roots are at $z = -1$. The other factor is the polynomial which contains free parameters. We refer to this factor as the free-polynomial. The coefficients of the free-polynomial are the free parameters. The SLF is also defined as a symmetric polynomial which can be expressed as a product of a binomial factor and a remainder polynomial. The coefficients of the remainder polynomial are obtained in terms of free parameters by solving a set of linear equations. (iii) We derive the system of linear equations from the half band condition on the product filter. The condition states that all coefficients corresponding to even powers of z of the product poly-

nomial should be zero except the constant term. Subsequently, the system of equations is solved and all filter coefficients are expressed in terms of free parameters. (iv) Finally, these free parameters are optimized to obtain FBs that yield time–frequency optimized discrete wavelet bases. Having obtained time–frequency localized WFBs, we employ the optimized FBs in an image coding application, for their performance evaluation and comparison with popular FBs.

The salient features of the proposed parametrization technique can be summarized as follows:

- The proposed parametrization technique is general and less restrictive than the existing parametrization based techniques [24,25]. We can design FBs of any order with the desired number of free parameters and VMs. This approach also avoids the factorization of the product polynomial, unlike the method of [17,35].
- We have explicitly obtained parametric expressions of analysis and synthesis filters of higher order FBs. These parametrized filter coefficients can be easily optimized, as there is no restriction on the free parameters.
- The optimality criterion takes into account JTFL of all discrete-time wavelet bases for the given number of decomposition levels. Further, we consider three different objective functions to obtain the desired time–frequency localized FBs.
- In the image coding application, the performance of the designed JTFL optimized FBs has been found better than the popular equivalent Cohen–Daubechies–Feauveau (CDF) FBs [19] as well as a previously designed JTFL optimized FBs by Sharma et al. [10].

2. Problem formulation

Fig. 1 depicts a typical two-channel biorthogonal FB [23] where $H_0(z)$ and $F_0(z)$ are ALF and SLF, respectively. $H_1(z)$ and $F_1(z)$ represent analysis high-pass filter and synthesis high-pass filter, respectively. Defining the product filter as

$$P(z) = z^l H_0(z) F_0(z) \tag{1}$$

where l is an odd integer, the expression for perfect reconstruction (half band) condition becomes [23],

$$P(z) + P(-z) = 2 \tag{2}$$

The product filter $P(z)$ is a symmetric (zero phase) polynomial expansion whose coefficients corresponding to even powers of z are zero, except for the term (z^0) which carries a coefficient 1. The filter $P(z)$ is also known as half band filter. Hence, the design of two-channel PR FB reduces to the design of a half band filter $P(z)$. In case of two-channel FBs the PR condition is equivalent to the biorthogonality condition [1,23]. Let us consider the LHBP, $P(z)$, which has a maximum number of zeros at $z = -1$ (zeros at $z = -1$ are referred to as VMs)

$$P_{4m-2}(z) = z^m (1 + z^{-1})^{2m} R_{2m-2}(z) \tag{3}$$

where

$$R_{2m-2}(z) = \left\{ \sum_{n=0}^{m-1} \binom{m+n-1}{n} (2 - z - z^{-1})^n \right\} \tag{4}$$

In (3) and (4), the subscripts denote the orders of the polynomials.

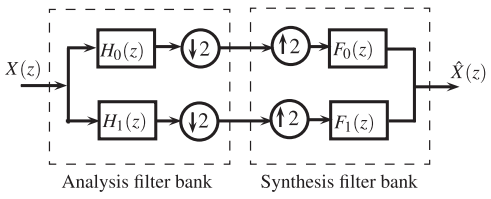

Fig. 1. Two-channel FB.

Popular CDF [19] biorthogonal WFBs are designed by factorizing a LHBP. The LHBP in (3) of the order $4m - 2$ has maximum $2m$ number of VMs. Thus, the LHBP does not provide any freedom for the optimization.

In this paper, our objective is to obtain some independent (free) parameters that can be optimized to design the time–frequency localized wavelet bases. In order to achieve some degrees of freedom, we first define the modified LHBP polynomial by freeing $2f$ number of zeros at $z = -1$ of the LHBP (3) as follows:

$$\check{P}_{4m-2}(z) = z^{(m-f)}(1 + z^{-1})^{2(m-f)} F_{2f}(z) Q_{2m-2}(z) \tag{5}$$

$$\check{P}_{4m-2}(z) = z^{(m-f)}(1 + z^{-1})^{2(m-f)} \check{R}_{2m+2f-2}(z) \tag{6}$$

where

$$\check{R}_{2m+2f-2}(z) = F_{2f}(z) Q_{2m-2}(z) \tag{7}$$

and

$$F_{2f}(z) = 1 + \sum_{n=1}^{f} a_n (z^n + z^{-n}) \tag{8}$$

$$Q_{2m-2}(z) = 1 + \sum_{n=1}^{m-1} b_n (z^n + z^{-n}) \tag{9}$$

where a_n and b_n are real coefficients. It is evident from (6) that the modified LHBP has $2(m - f)$ VMs.

The polynomial $F(z)$ is an arbitrary (symmetric) polynomial of degree $2f$, such that $F(-1) \neq 0$ and $f \in \{1, 2, 3, \ldots, m-1\}$. Eq. (7) indicates that the remainder polynomial, $\check{R}(z)$, corresponding to the modified LHBP (6) consists of two factors, $F(z)$ and $Q(z)$. The polynomial $F(z)$ in (8) contains free (independent) parameters. The symmetric polynomial $Q_{2m-2}(z)$ in (9) of degree $2m - 2$, contains $m - 1$ unknown coefficients b_n. Subsequently, we shall refer the polynomial $F(z)$ as the free polynomial, as it gives some degrees of freedom in designing the FB. Note, $F(z)$ denotes the free polynomial, whereas $F_0(z)$ represents the SLF. The parameter f represents number of degrees of freedom. The case corresponding to f=0 turns the modified LHBP (6) back to the LHBP (3), which has no freedom. The modified LHBP (6) corresponding to maximum number of freedoms, $f = m - 1$, yields an irregular FB, the one which does not have any VMs. Hence, the FB cannot be regarded as a valid candidate of a wavelet FB. Thus for the given order, $4m - 2$, of the modified LHBP, the maximum possible number of free parameters is $m - 2$ instead of $m - 1$ which in turn excludes the possibility of irregular filters.

3. Problem solution

In this section, we demonstrate the proposed method to obtain linear phase, two-channel FBs with prescribed number of VMs and degrees of freedom. Since, we are designing linear phase filters, it is more convenient to use the variable $y = \frac{(z+z^{-1})}{2}$. The change of variables embeds the linear phase in the structure itself. The change of variables reduces the orders of polynomials by a factor of half. Thus, the modified LHBP in the variable y can be given as,

$$\widetilde{P}_{2m-1}(y) = (1 + y)^{(m-f)} \widetilde{F}_f(y) \widetilde{Q}_{m-1}(y) = (1 + y)^{(m-f)} \widetilde{R}_{m+f-1}(y) \tag{10}$$

The PR condition on the polynomial $\widetilde{P}(y)$ can be stated as $\check{P}(y) + \check{P}(-y) = 2$; i.e., the coefficients of even powers of y are zero except the constant term. It is evident that out of total $2m - 1$ degrees of freedom, $m - f$ degrees of freedom are used to assign VMs (regularity) and $m - 1$ degrees of freedom are exhausted in satisfying PR (half-band) conditions. Hence, we are left with f degrees of freedom that can be used to optimize wavelet filter coefficients. Besides, VMs (regularity) can be traded for increased degrees of freedom. In the proposed method, we need not factorize the product filter. Instead, we a priori choose the lengths and numbers of VMs for both analysis as

Table 1
Three classes of FBs with one, two and three free parameters for m=5.

Name	Free parameters	VMs	Equations
9/11	α, β, γ	(2,2)	Refer Eqs. (25)–(28)
10/10	α, β, γ	(3,1)	
8/12	α, β, γ	(1,3)	
9/11	α, β	(4,2)	$q_1 = -\alpha - 3$
10/10	α, β	(5,1)	$q_2 = (96\alpha + 18\alpha^2\beta^2 + 48\alpha\beta + 144\alpha^2 + 96\alpha^3 + 24\alpha^4 + 19\alpha\beta^2 + 81\alpha^2\beta + 3\alpha\beta^3 + 35\alpha^3\beta + 24)/\Lambda_2$
7/13	α, β	(2,4)	$q_3 = (-48\alpha - 35\alpha^2\beta^2 - 48\alpha\beta - 96\alpha^2 - 80\alpha^3 - 24\alpha^4 - 33\alpha\beta^2 - 96\alpha^2\beta - 9\alpha\beta^3 - 48\alpha^3\beta - 8)/\Lambda_2$
8/12	α, β	(3,3)	$q_4 = (8\alpha + 24\alpha^2\beta^2 + 24\alpha\beta + 24\alpha^2 + 24\alpha^3 + 8\alpha^4 + 24\alpha\beta^2 + 48\alpha^2\beta + 8\alpha\beta^3 + 24\alpha^3\beta)/\Lambda_2$
6/14	α, β	(1,5)	where $\Lambda_2 = 24\alpha + 11\alpha\beta + 24\alpha^2 + 8\alpha^3 + 3\alpha\beta^2 + 9\alpha^2\beta + 8$
9/11	α	(6,2)	$q_1 = -\alpha - 4$
10/10	α	(7,1)	$q_2 = (20\alpha^4 + 109\alpha^3 + 232\alpha^2 + 233\alpha + 96)/\Lambda_3$
7/13	α	(4,4)	$q_3 = -(29\alpha^4 + 132\alpha^3 + 233\alpha^2 + 192\alpha + 64)/\Lambda_3$
6/14	α	(3,5)	$q_4 = (16\alpha^4 + 64\alpha^3 + 96\alpha^2 + 64\alpha + 16)/\Lambda_3$
5/15	α	(2,6)	where $\Lambda_3 = 5\alpha^3 + 20\alpha^2 + 29\alpha + 16$
4/16	α	(1,7)	
8/12	α	(5,3)	

well as synthesis filters, and both are explicitly obtained in terms of the free parameters. Let us consider zero phase odd-length analysis and synthesis low pass filters $H_0(z)$ and $F_0(z)$:

$$F_0(z) = z^{v}(1 + z^{-1})^{2v}Q_{2m-2}(z) \tag{11}$$

$$H_0(z) = z^{(m-f-v)}(1 + z^{-1})^{2(m-f-v)}F_{2f}(z) \tag{12}$$

The orders of the synthesis and analysis filters are chosen $2(m + v - 1)$ and $2(m - v)$, respectively. The respective numbers of VMs imposed on the analysis and synthesis filters are $2(m - f - v)$ and $2v$, where $v \in \{1, 2, 3, \ldots, m - 2\}$. By substituting $y = \frac{(z+z^{-1})}{2}$ and using Chebyshev polynomials, in Eqs. (11) and (12), we obtain

$$\widetilde{F}_0(y) = (1 + y)^{v}\widetilde{Q}_{m-1}(y) \tag{13}$$

$$\widetilde{H}_0(y) = (1 + y)^{m-f-v}\widetilde{F}_f(y) \tag{14}$$

where the polynomials $\widetilde{F}_f(y)$ and $\widetilde{Q}_{m-1}$ are given by

$$\widetilde{F}_f(y) = y^{f} + \sum_{i=1}^{f} \alpha_i y^{f-i} \tag{15}$$

$$\widetilde{Q}_{m-1}(y) = y^{m-1} + \sum_{k=1}^{m-1} q_k y^{m-1-k} \tag{16}$$

The parameters $\alpha_i \in \mathbb{R}$ are free (independent) parameters and q_k are unknown real coefficients. We obtain q_k in terms of α_i via solving the determined system of $(m - 1)$ linear equations that are obtained from the half band (PR) conditions. Thus, we express both polynomials $\widetilde{H}_0(y)$ and $\widetilde{F}_0(y)$ in terms of the free parameters α_i. The ALF and SLF $H_0(z)$ and $F_0(z)$ can be obtained, explicitly in terms of free parameters, by substituting back $y = \frac{z+z^{-1}}{2}$ in the parametric expressions of the polynomials $\widetilde{H}_0(y)$ and $\widetilde{F}_0(y)$, respectively.

The aforementioned method illustrates the design of the odd-length FB comprising the analysis and synthesis filters with the lengths $2(m - v)$ and $2(m + v - 1)$, respectively, where the filters have f degrees of freedom. For the given value of m, we can obtain different odd-length FBs by varying the value of $v \in \{1, 2, 3, \ldots, m - 2\}$. The filters can have different numbers of free parameters $f \in \{1, 2, 3, \ldots, m - 2\}$. For the given m, we obtain $\frac{(m-1)(m-2)}{2}$ distinct odd-length FBs. The even-length FBs are also obtained from the re-factorization of designed odd-length FBs. In the process of re-factorization, a factor $(z + 1)^{p}$, where p is an odd integer, is multiplied with (or divided from) the ALF and the same factor is divided from (or multiplied with) the SLF. Since, the PR condition remains intact during the process of re-factorization, the relation between free parameter α_i and unknown coefficients q_k also remains unaltered. For the given m, we design $\frac{(m+1)(m-2)}{2}$ distinct even-length FBs. Thus, we can obtain total $m(m - 2)$ different regular FBs, for the given m. The regular FB refers to the one whose both ALF and SLF have at least one zero at $z = -1$.

4. Construction of parametric FB families

The proposed method is fairly general to design almost any biorthogonal FB. We illustrate the method via the following design examples. First, we choose the desired value of m, which fixes the order of the modified LHBP. Let us consider the modified LHBP with m=5 which fixes the order of the polynomial to $4m - 2 = 18$:

$$\check{P}_{18}(z) = z^{(5-f)}(1 + z^{-1})^{2(5-f)}F_{2f}(z)Q_8(z) \tag{17}$$

Using Chebyshev polynomials and the change of variable, $y = \frac{(z+z^{-1})}{2}$, in (17) provides the following expression of the LHBP in the variable y:

$$\widetilde{P}_9(y) = (1 + y)^{5-f}\widetilde{F}_f(y)\widetilde{Q}_4(y) \tag{18}$$

where the number of free parameters $f \in \{1, 2, 3\}$. Thus, we can design three different families of FBs comprising fifteen distinct FBs with one, two and three parameters (Table 1). We now design all three classes of FBs having three, two and one free parameters, respectively. From this point onwards, we shall consider all polynomials (filters) in terms of variable y.

4.1. Construction of parametric FBs with 3 free parameters

By choosing f=3, we free six VMs of the LHBP. Thus the modified LHBP has 4 VMs. The filter pair of lengths 9 and 11 can be designed by assigning a pair of VMs to ALF as well as SLF. The ALF and SLF can be expressed in terms of variable y as:

$$\widetilde{H}_0(y) = (1 + y)\widetilde{F}_3(y) \tag{19}$$

$$\widetilde{F}_0(y) = (1 + y)\widetilde{Q}_4(y) \tag{20}$$

where

$$\widetilde{F}_3(y) = y^3 + \alpha y^2 + \beta y + \gamma \tag{21}$$

$$\widetilde{Q}_4(y) = y^4 + q_1y^3 + q_2y^2 + q_3y + q_4 \tag{22}$$

Note that the order of $\widetilde{H}_0(y)$ and $\widetilde{F}_0(y)$ in (19) and (20) are 4 and 5, respectively. Both $\widetilde{H}_0(y)$ and $\widetilde{F}_0(y)$, have a zero at $y = -1$, which in turn implies that both $H_0(z)$ and $F_0(z)$ have a pair of zeros at $z = -1$. We have four unknown coefficients q_1, q_2, q_3 and q_4 and three free parameters $\{\alpha,\ \beta,\ \gamma\}$. The product filter $\widetilde{P}(y)$ can be given by

$$\widetilde{P}(y) = (1+y)^2\widetilde{F}_3(y)\widetilde{Q}_4(y) \tag{23}$$

unknown coefficients $\{q_1, q_2, q_3, q_4\}$ are obtained in terms of free parameters using the half band condition [23]. Applying half band (PR) condition, the coefficients of y^2, y^4, y^6 and y^8 in the polynomial $\widetilde{P}(y)$ of (23) are equated to zero. This gives the following set of 4 linear equations:

$$\begin{aligned} q_1 + \alpha + 2 &= 0q_1 + 2q_2 + q_3 + \alpha(2q_1 + q_2 + 1) + (q_1 + 2)\beta + \gamma \\ &= 0q_3 + 2q_4 + \gamma(2q_1 + q_2 + 1) + \alpha(q_2 + 2q_3 + q_4) \\ &\quad + \beta(q_1 + 2q_2 + q_3) = 0\alpha q_4 + (q_3 + 2q_4)\beta + \gamma(q_2 + 2q_3 + q_4) \\ &= 0 \end{aligned} \tag{24}$$

On solving the set of equations in (24), we obtain

$$q_1 = -2 - \alpha \tag{25}$$

$$\begin{aligned} q_2 = (&-8\beta^2\alpha^2 + 6\gamma\beta - 2\alpha + 6\gamma - 10\beta\alpha^3 - \gamma\beta^2\alpha - 2\alpha\beta^3 - 2\alpha^2\beta\gamma - 8\alpha^2 \\ &+ 16\alpha\gamma \quad - 6\alpha\beta - 16\alpha^2\beta + 8\gamma\beta\alpha - 6\beta^2\alpha + 2\gamma\beta^2 + \gamma^2\beta + 2\gamma^2\alpha \\ &+ 10\gamma\alpha^2 - 10\alpha^3 - 4\alpha^4)/\Lambda_1 \end{aligned} \tag{26}$$

$$\begin{aligned} q_3 = (&-\gamma^3 - 4\gamma^2\alpha + \gamma^2\beta\alpha - 4\gamma^2\beta - 2\gamma^2 - 8\gamma\alpha^2 + 4\alpha^2\beta\gamma - 8\gamma\beta\alpha + 4\gamma\beta^2\alpha \\ &- 12\alpha\gamma - 4\gamma \quad - 8\gamma\beta - 4\gamma\beta^2 + 2\alpha^4 + 4\alpha^3 + 8\beta\alpha^3 + 2\alpha^2 + 12\alpha^2\beta \\ &+ 10\beta^2\alpha^2 + 4\alpha\beta + 4\alpha\beta^3 + 8\beta^2\alpha)/\Lambda_1 \end{aligned} \tag{27}$$

$$\begin{aligned} q_4 = (&4\gamma^2\beta + 4\gamma\beta + 2\gamma\beta^2 - 2\alpha\beta + 4\gamma^2\alpha - 2\alpha\beta^3 - 4\beta^2\alpha^2 + 2\gamma\alpha^2 + 4\gamma^2 \\ &- 2\beta\alpha^3 + 4\alpha\gamma \quad - 4\alpha^2\beta\gamma - 4\beta^2\alpha - 4\alpha^2\beta - 2\gamma^2\beta\alpha - 4\gamma\beta^2\alpha + 2\gamma \\ &+ 2\gamma^3)/\Lambda_1 \end{aligned} \tag{28}$$

where

$$\Lambda_1 = 4\alpha\gamma - 4\alpha\beta + 4\gamma - 4\alpha^2\beta - 2\alpha + \gamma^2 - 2\beta^2\alpha - 2\alpha^3 - 4\alpha^2 - \gamma\beta\alpha + 2\gamma\beta$$

Thus, we have both polynomials $\widetilde{H}_0(y)$ and $\widetilde{F}_0(y)$ in terms of free parameters (α, β, γ) (Table 2). On substituting back, $y = \frac{z+z^{-1}}{2}$ in these polynomials, we get the desired parameterized filters.

Important remarks: Before exemplifying the design of FBs with two free parameters, the salient and distinct features of the aforementioned parametric construction are highlighted as follows:

(i) By choosing different values of free parameters, one can obtain different 9/11 FB. Interestingly, we have derived the original CDF-9/11 [19] FB by the following choice of free parameters $\{\alpha = -2.10013469,\ \beta = -0.5894783,\ \gamma = 2.5106546\}$.

(ii) Tay [24] attempted to design the 9/11 parameterized FB. But, the author did not present free parameter based expressions of the analysis and synthesis filters. In this work, we have presented the parametrized expressions of the filters for the 9/11 and 10/10 FBs.

(iii) Recently Murugesan and Tay [25] also designed a 9/11 FB, with two free parameters using a restrictive design technique in which the VMs can be reduced only in one filter (either ALF or SLF) but not in both. The important feature of the proposed design is that the reduction of VMs is permissible for both filters, simultaneously. Hence, the proposed technique provides more freedom and flexibility than the technique of Murugesan and Tay [25]. Also the reduction of VMs occurs for both filters unlike the method of Murugesan and Tay [25]. The original CDF-9/11 FB has ALF and SLF with 4 and 6 VMs. In the above design, we have reduced 2 and 4 VMs from ALF and SLF, respectively. Thus we obtained three degrees of freedom.

Table 2
Filter coefficients: 9/11 FB with 3 free parameters.

n	$h_0(n)$	$f_0(n)$
0	$\frac{\alpha}{2} + \frac{\beta}{2} + \gamma + \frac{3}{8}$	$\frac{3}{8}q_1 + \frac{q_2}{2} + \frac{q_3}{2} + q_4 + \frac{3}{8}$
±1	$\frac{3}{8}\alpha + \frac{\beta}{2} + \frac{\gamma}{2} + \frac{3}{8}$	$\frac{3}{8}q_1 + \frac{3}{8}q_2 + \frac{q_3}{2} + \frac{q_4}{2} + \frac{5}{16}$
±2	$\frac{\alpha}{4} + \frac{\beta}{4} + \frac{1}{4}$	$\frac{q_1}{4} + \frac{q_2}{4} + \frac{q_3}{4} + \frac{1}{4}$
±3	$\frac{\alpha}{8} + \frac{1}{8}$	$\frac{q_1}{8} + \frac{q_2}{8} + \frac{5}{32}$
±4	$\frac{1}{16}$	$\frac{q_1}{16} + \frac{1}{16}$
±5		$\frac{1}{32}$

4.2. Construction of parametric FBs with two free parameters

By setting f=2, four VMs from the LHBP has been reduced. Thus, the modified LHBP has now 6 VMs. The filter pair of lengths 7 and 13 can be designed by assigning 2 and 4 VMs to ALF and SLF, respectively. The modified ALF and SLF can be expressed as

$$\widetilde{H}_0(y) = (1+y)(y^2 + \alpha y + \beta) \tag{29}$$

$$\widetilde{F}_0(y) = (1+y)^2(y^4 + q_1y^3 + q_2y^2 + q_3y + q_4) \tag{30}$$

An alternative filter pair of lengths 9 and 11, with 4 and 2 VMs for ALF and SLF, respectively can be expressed as follows:

$$\widetilde{H}_0(y) = (1+y)^2(y^2 + \alpha y + \beta) \tag{31}$$

$$\widetilde{F}_0(y) = (1+y)(y^4 + q_1y^3 + q_2y^2 + q_3y + q_4) \tag{32}$$

Similar to the case of 3 free parameters, we formulate a determined system of 4 linear equations that are obtained from the PR (half band) condition. By solving the set of equations, we represent coefficients $\{q_1, q_2, q_3, q_4\}$ in terms of two free parameters $\{\alpha, \beta\}$ as shown in Table 1.

4.3. Construction of parametric FBs with one free parameter

The choice f=1 relaxes two VMs of the LHBP. Thus, the modified LHBP has now 8 VMs. By assigning 2 and 6 VMs to ALF and SLF, respectively, the filter pair of lengths 5 and 15 can be defined as follows:

$$\widetilde{H}_0(y) = (1+y)(y+\alpha) \tag{33}$$

$$\widetilde{F}_0(y) = (1+y)^3(y^4 + q_1y^3 + q_2y^2 + q_3y + q_4) \tag{34}$$

In case of one free parametrized construction, there are two more alternatives for defining the filters as follows. By assigning 4 VMs each to ALF and SLF, respectively, a filter pair of lengths 7 and 13 can be designed as

$$\widetilde{H}_0(y) = (1+y)^2(y+\alpha) \tag{35}$$

$$\widetilde{F}_0(y) = (1+y)^2(y^4 + q_1y^3 + q_2y^2 + q_3y + q_4) \tag{36}$$

We assign 6 and 2 VMs to ALF and SLF, respectively, in this case the filter pair of lengths 9 and 11 can be designed as follows:

$$\widetilde{H}_0(y) = (1+y)^3(y+\alpha) \tag{37}$$

$$\widetilde{F}_0(y) = (1+y)(y^4 + q_1y^3 + q_2y^2 + q_3y + q_4) \tag{38}$$

The coefficients $\{q_1, q_2, q_3, q_4\}$ can be obtained in terms of the free parameter α, as given in Table 1, by solving a set of 4 linear equations in similar manner as that of three and two parameters cases.

Hence, with m=5, we have designed three different families of FBs with one, two and three free parameters. We have thus designed total 15 different regular wavelet FBs, out of which 6 FBs have an odd length and the remaining 9 FBs have an even-length. The details about these FB designs are given in Table 1. In the subsequent section, we present a method to obtain JTFL wavelet bases via optimizing the free parameters of the designed filter pairs.

5. Time–frequency localization and discrete wavelet bases

The uncertainty principle prevents arbitrary localization of a signal in time and frequency domains, simultaneously. Ishii and Furukawa [36] have proposed a variance based time–frequency localization measure for sequences in $l_2(\mathbb{Z})$. Let $h(n)$ be a discrete-time real valued sequence in $l_2(\mathbb{Z})$ with $|h|_2^2 = 1$. Let $H(e^{j\omega})$ be its discrete-time Fourier transform (DTFT). The time variance σ_n^2 of the sequence, along with its time mean n_0, can be given as follows:

$$n_0 = \sum_{n\in\mathbb{Z}} n|h(n)|^2\sigma_n^2 = \sum_{n\in\mathbb{Z}} (n-n_0)^2|h(n)|^2 \tag{39}$$

For a low-pass sequence $h(n)$, frequency mean ω_0 and frequency variance σ_ω^2 can be given by

$$\omega_0 = 0\sigma_\omega^2 = \frac{1}{2\pi}\int_{-\pi}^{\pi}(\omega-\omega_0)^2|H(\omega)|^2 d\omega \tag{40}$$

Let Δ_h denote the product of time and frequency variances of the sequence $h(n)$. The Δ_h is referred to as time–frequency product (TFP) of the sequence $h(n)$. The uncertainty principle imposes a lower bound on the TFP. The following inequality represents the lower bound [37]:

$$\Delta_h = \sigma_n^2\sigma_\omega^2 \geq \frac{(1-|H(\pi)|)^2}{4} \tag{41}$$

For a band-pass sequence $h(n)$, one-sided frequency mean ω_0 and frequency variance σ_ω^2 can be given by [37]:

$$\omega_0 = \frac{1}{\pi}\int_0^{\pi}\omega|H(\omega)|^2 d\omega\sigma_\omega^2 = \frac{1}{\pi}\int_0^{\pi}(\omega-\omega_0)^2|H(\omega)|^2 d\omega \tag{42}$$

Following (39) and (42), TFP of a band-pass sequence is lower bounded as given by the following inequality [37]:

$$\Delta_h = \sigma_n^2\sigma_\omega^2 \geq \frac{(1-\mu)^2}{4} \tag{43}$$

where

$$\mu = \frac{\omega_0}{\pi}|H(0)|^2 + \left(1-\frac{\omega_0}{\pi}\right)|H(\pi)|^2$$

For a high-pass sequence $h(n)$, frequency mean ω_0 and frequency variance σ_ω^2 can be given by [37]

$$\omega_0 = \pi\sigma_\omega^2 = \frac{1}{2\pi}\int_{-\pi}^{\pi}(\omega-\omega_0)^2|H(\omega)|^2 d\omega \tag{44}$$

Thus using (39) and (44) TFP for a high-pass sequence can be given by [37]

$$\Delta_h = \sigma_n^2\sigma_\omega^2 \geq \frac{(1-|H(0)|)^2}{4} \tag{45}$$

For all the three cases corresponding to low-pass, high-pass and band-pass sequences, the TFP of a sequence in $l_2(\mathbb{Z})$ is also lower bounded similar to the case of continuous-time functions in $L_2(\mathbb{R})$. This happens if the spectrum of the sequence vanishes at $\omega=\pi$ and/or $\omega=0$. In our designs, both the ALF and SLF have at least one zero at $\omega=\pi$. Also, both the analysis and synthesis high-pass filters have at least one zero at $\omega=0$ and all the band pass discrete wavelet sequences, which are generated through iterations of the ALF and SLF have at least one zero at $\omega=\pi$ and one at $\omega=0$. Therefore, the TFP of all filters and sequences designed by us is lower bounded by 0.25, which can be expressed as follows:

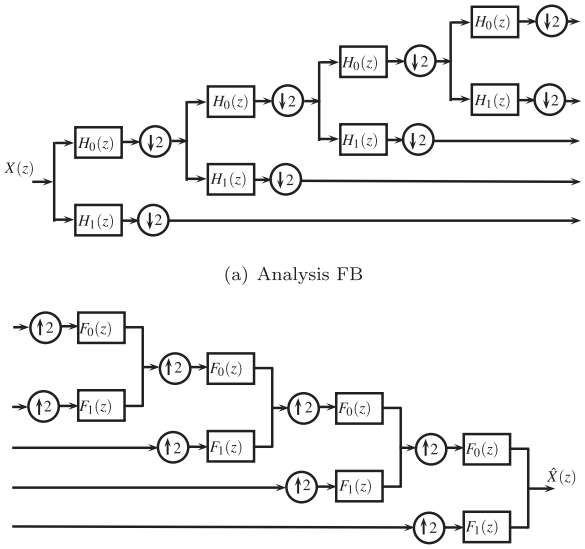

(a) Analysis FB

(b) Synthesis FB

Fig. 2. Tree-structured FBs.

$$\Delta_h = \sigma_n^2\sigma_\omega^2 \geq \tfrac{1}{4} \tag{46}$$

We consider J number of iterations of the typical two channel biorthogonal FB (Fig. 1) to decompose a signal into $J+1$ subbands. Figs. 2(a) and (b) show the tree-structured analysis and synthesis FBs, respectively, for the case J=4. Using noble identities [2], the J-level tree-structured iterated FB can be transformed into an equivalent parallel-structured FB consisting of $J+1$ parallel filters, as shown in Fig. 3. Note that, out of the $J+1$ parallel filter branches, the topmost branch is a low pass filter; the bottommost branch is a high pass filter and the others are band pass filters. In our optimization problem, we minimize TFP not only of the low pass filter, but also of all band pass filters and the high pass filters of the $J+1$ parallel filters.

The $J+1$ analysis filters of the parallel-structured FB can be given by the following expressions:

$$H_1^1(z) = H_1(z)H_1^i(z) = H_1(z^{2^{i-1}})\prod_{k=0}^{i-2}H_0(z^{2^k}),$$
$$i = 2, 3, \ldots, J H_0^J(z) = \prod_{k=0}^{J-1}H_0(z^{2^k}) \tag{47}$$

The $J+1$ synthesis filters can be represented as follows:

$$F_1^1(z) = F_1(z)F_1^i(z) = F_1(z^{2^{i-1}})\prod_{k=0}^{i-2}F_0(z^{2^k}),$$
$$i = 2, 3, \ldots, J F_0^J(z) = \prod_{k=0}^{J-1}F_0(z^{2^k}) \tag{48}$$

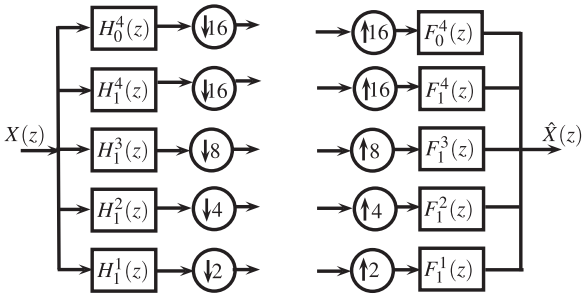

(a) Analysis FB (b) Synthesis FB

Fig. 3. Parallel-structured FBs.

Let $h_1^i(n)$, $i = 1. \ldots, J$, and h_0^J be the time domain representations (impulse response sequences) of the $J + 1$ parallel filters of the parallel-structured analysis FB. These sequences are subsequently referred to as wavelet vectors or wavelet sequences. The set of these vectors is called discrete-time analysis wavelet basis, and is denoted by Ψ. Similarly, let $f_1^i(n)$, $i = 1. \ldots, J$, and f_0^J represent impulse response sequences corresponding to the $J + 1$ parallel filters of the parallel-structured synthesis FB. These sequences are referred to as synthesis wavelet vectors. The set of the sequences forms the discrete-time synthesis wavelet basis which is denoted by $\widetilde{\Psi}$.

We now extend time–frequency localization properties of an individual sequence to the collective localization properties of discrete wavelet bases defined above. The uncertainty principle, therefore, can also be extended to the discrete-time analysis and synthesis bases. Let $\eta = \{h_1, h_2, h_3, \ldots h_N\}$ be a basis that contains N discrete wavelet vectors, h_k. For the basis η, we now introduce TFP which is given by,

$$\Delta_\eta = \sum_{k=1}^{N} w_k \Delta_{h_k} \tag{49}$$

where w_k are the weights such that $0 \le w_k \le 1$ and $\sum_{k=1}^{N} w_k = 1$. It follows from (49) that Δ_η is a weighted average of the TFPs of the basis vectors of the basis η. For the sequence h_k, following (46), we have the inequality $\Delta_{h_k} = \sigma_n^2 \sigma_\omega^2 \ge \frac{1}{4}$. This leads to the following uncertainty relation for the basis η:

$$\Delta_\eta = \frac{1}{N} \sum_{k=1}^{N} \Delta_{h_k} \ge \frac{1}{4} \tag{50}$$

Hence, the TFP of discrete-time analysis and synthesis wavelet bases is also lower bounded by 0.25, similar to the case of continuous-time bases and functions.

6. Optimization method

In this paper, our objective is to obtain time–frequency localized discrete-time wavelet bases. For this we minimize the following objective function:

$$\Phi = \rho \Delta_\Psi + (1 - \rho)\Delta_{\widetilde{\Psi}}, \quad \rho \in [0, 1] \tag{51}$$

where Δ_Ψ and $\Delta_{\widetilde{\Psi}}$ are TFPs of the discrete-time analysis and synthesis wavelet basses, respectively. ρ is a trade-off factor for controlling localizations of analysis and synthesis bases. In this work, the following three different cases corresponding to $\rho = 1$, 0 and 0.5 have been considered to obtain time–frequency optimized wavelet bases:

1. *Optimal analysis wavelet basis*: In the first case corresponding to $\rho = 1$, we minimize the TFP of analysis wavelet basis for J levels of iterations. The objective function can be given as follows:

$$\Phi = \Delta_\Psi = w_1 \Delta_{h_1^1} + w_2 \Delta_{h_1^2} + \cdots + w_J \Delta_{h_1^J} + w_{J+1} \Delta_{h_0^J} \tag{52}$$

where $\Delta_{h_1^1}, \Delta_{h_1^2}, \ldots, \Delta_{h_1^J}, \Delta_{h_0^J}$ are TFPs of the basis vectors of the analysis wavelet basis Ψ.

2. *Optimal synthesis wavelet basis*: In the second case corresponding to $\rho = 0$, we minimize the TFP of the discrete-time synthesis wavelet basis. The objective function can be expressed as follows:

$$\Phi = \Delta_{\widetilde{\Psi}} = w_1 \Delta_{f_1^1} + w_2 \Delta_{f_1^2} + \cdots + w_J \Delta_{f_1^J} + w_{J+1} \Delta_{f_0^J} \tag{53}$$

where $\Delta_{f_1^1}, \Delta_{f_1^2}, \ldots, \Delta_{f_1^J}, \Delta_{f_0^J}$ represent TFPs of basis vectors of the synthesis basis, $\widetilde{\Psi}$.

3. *Jointly optimal analysis and synthesis wavelet bases*: In the third case corresponding to $\rho = 0.5$, we minimize the TFP of the analysis and synthesis wavelet bases jointly. The objective function is given by following expression:

$$\Phi = \Delta_{\Psi + \widetilde{\Psi}} = \frac{1}{2}\{\Delta_\Psi + \Delta_{\widetilde{\Psi}}\} \tag{54}$$

Table 3
TFPs of odd-length optimal wavelet bases.

FB	Optimal free parameter values	Δ_Ψ	$\Delta_{\widetilde{\Psi}}$	$\Delta_{\Psi+\widetilde{\Psi}}$
A_2-11/9	−5.7445, 6.7078	0.3807	0.5401	0.4604
B_2-11/9	−4.8159, 6.7914	1.5283	0.3614	0.9449
C_2-11/9	−11.3907, 15.8622	0.4023	0.4512	0.4267
A_3-11/9	−2.7975, −13.7852, 38.6584	**0.3281**	1.6678	0.9979
B_3-11/9	−2.5297, 0.9980, 3.1318	1.2100	**0.3409**	0.7754
C_3-11/9	−8.0496, 3.5293, 10.7211	0.4106	0.4351	**0.4229**
CDF-11/9 [19]	–	0.4350	0.7071	0.5683
S-11/9 [10]	–	49.9783	0.5738	25.2760

The minimum value for each objective function is marked in bold.

Table 4
TFPs of even-length optimal wavelet bases.

FB	Optimal free parameter values	Δ_Ψ	$\Delta_{\widetilde{\Psi}}$	$\Delta_{\Psi+\widetilde{\Psi}}$
A_2-12/8	4.7890, −10.2297	0.3376	0.6793	0.5085
B_2-12/8	−0.3677, −2.4178	4.7731	0.4091	2.5911
C_2-12/8	1.2007, −4.8418	0.3688	0.5022	0.4355
A_3-12/8	10.5080, −6.2056, −34.6363	**0.3118**	2.4574	1.3846
B_3-12/8	4.50225, −8.4022, −10.3520	0.8777	**0.4034**	0.6405
C_3-12/8	2.5940, −3.8140,−4.8276	0.3707	0.4670	**0.4189**
CDF-12/8 [19]	–	3.7469	0.4448	2.0959

The minimum value for each objective function is marked in bold.

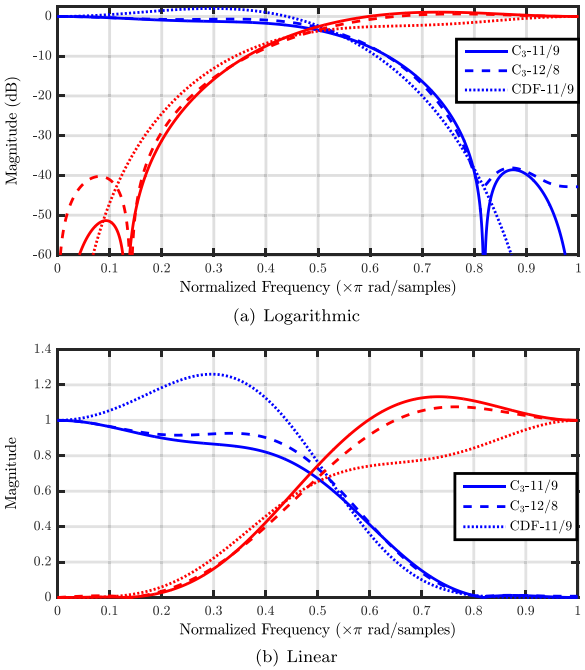

Fig. 4. Frequency responses of filter pair H_0, H_1 of optimal FBs C_3-11/9, C_3-12/8 and CDF-11/9.

Unconstrained optimization problem: Conditions of PR and VMs have been imposed structurally in the parametric construction of FBs. Thus, the design of time–frequency localized wavelet bases corresponding to each of the three cases can be expressed by the following unconstrained minimization problem:

$$(h_0^*(n), f_0^*(n)) = \underset{\{\alpha_i\}}{\operatorname{argmin}}(\Phi(\alpha_i)) \tag{55}$$

where Φ represents one of the following: $\Delta_{\widetilde{\Psi}}$, Δ_Ψ, $\Delta_{\Psi+\widetilde{\Psi}}$. $\{\alpha_i\}$ is the set of

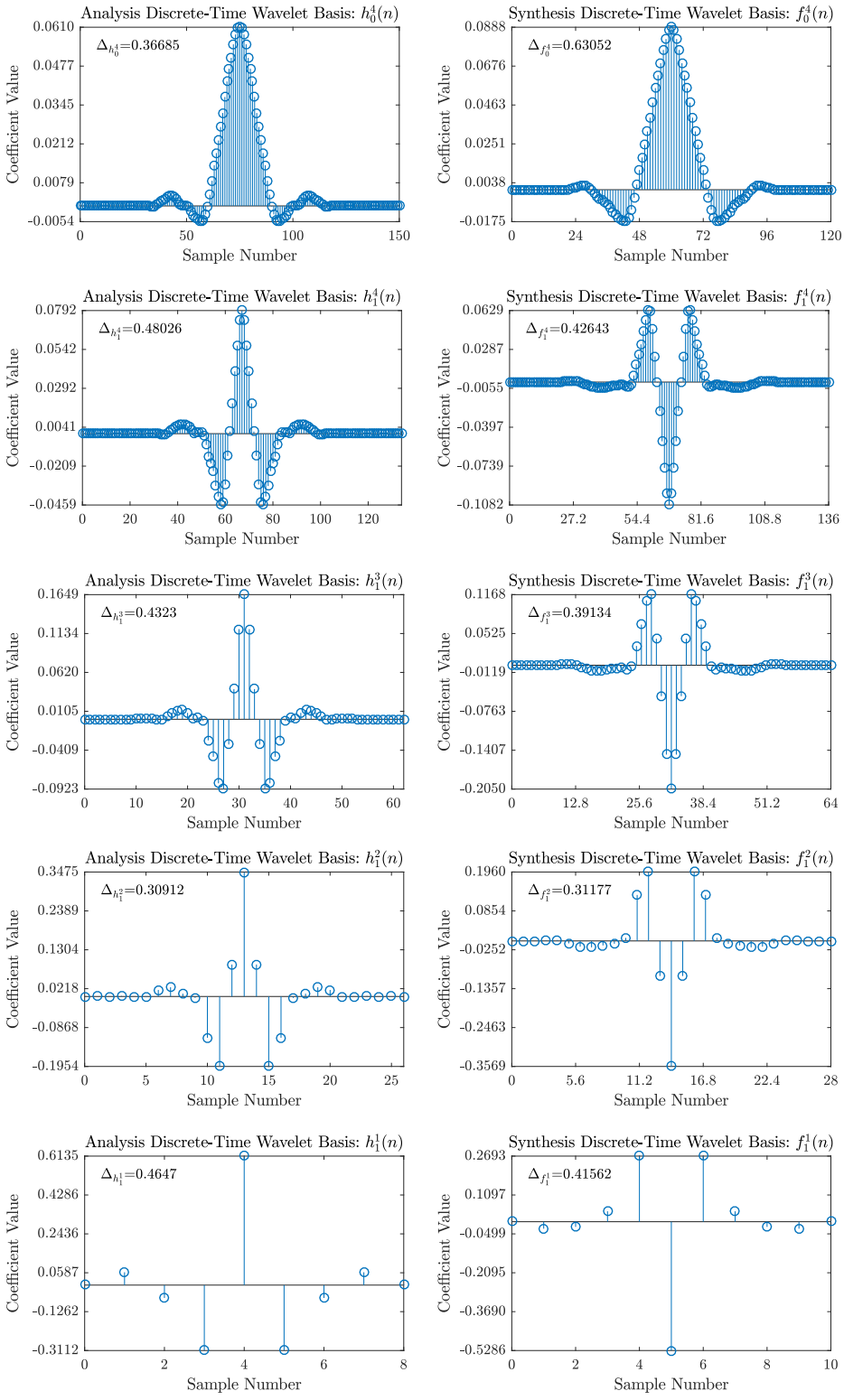

Fig. 5. Wavelet basis sequences of discrete-time analysis and synthesis bases of optimal FB C_3-11/9.

free parameters and $h_0^*(n)$ and $f_0^*(n)$ represent optimal ALF and SLF that yields optimal wavelet bases. We thereby get different $h_0^*(n)$ and $f_0^*(n)$ by following different optimization cases. Having obtained the optimal low-pass filters, optimal discrete-time analysis and synthesis wavelet bases can be generated as explained in Section 5. Note, the FBs are regular only over a certain range of values of free parameters, $\{\alpha_i\}$. Therefore, we first find the range of free parameter values over which the FBs obtained are regular wavelet FBs. Thus, we restrict the optimization process to search the solution in this range only. Further to ensure that the optimization process does not provide a local minimum, we run the optimization algorithm with different initial values of free parameters. This helps the algorithm to converge to at least a good minimum (near optimal) solution, if not the global solution. Thus, the strategy gives better solution compared to the case where the initial value is arbitrarily chosen. The entire optimization process can be explained by the following step by step procedure:

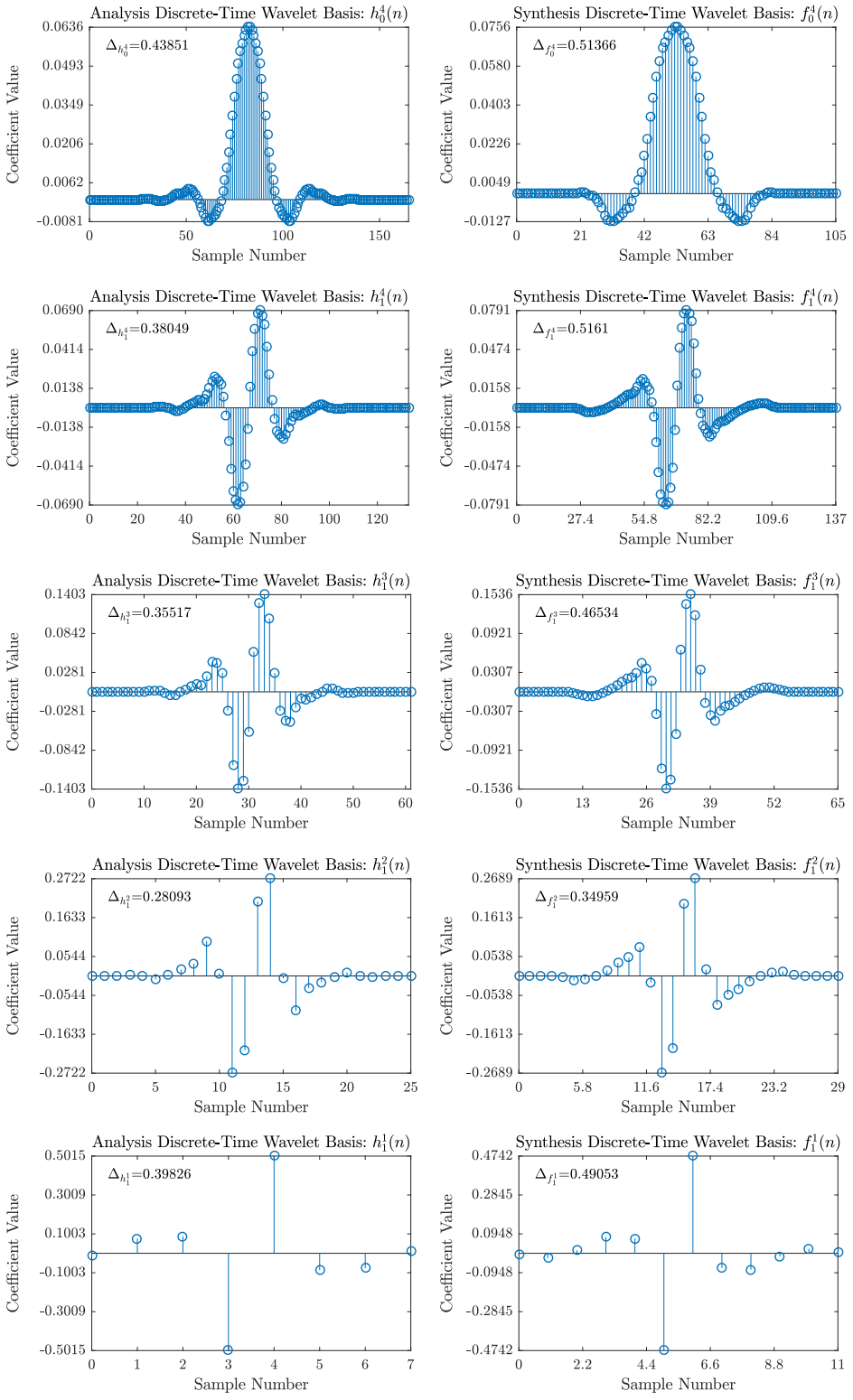

Fig. 6. Wavelet basis sequences of discrete-time analysis and synthesis bases of optimal FB C_3-12/8.

1. Fix the lengths, VMs and number of free parameters of the filter pair. Also, fix the number of levels of decomposition J.
2. Find parametric expressions of $H_0(z)$ and $F_0(z)$ using the proposed parametric technique in Section 4.
3. Find the region of free parameter values where the FBs are regular. The cascade algorithm converges in this region.
4. Select initial values for free parameters from the above mentioned range.
5. Perform the optimization using MATLAB optimization toolbox's *fmincon* solver with objective function being Φ in (55).
6. Check whether the value of the objective function returned by the solver is close to the lower bound 0.25. Else, go to step 4 and redo the optimization problem with a different initial value. Repeat the process for different initial values until the value of cost function converges close to 0.25 or the value of objective function does not vary with initial values.

Table 5
Time for computing optimal filters (in seconds).

Odd-length FB	Computation time	Even-length FB	Computation time
A_2-11/9	**0.0204**	A_2-12/8	0.0240
B_2-11/9	0.0222	B_2-12/8	0.0209
C_2-11/9	0.0224	C_2-12/8	0.0209
A_3-11/9	0.0303	A_3-12/8	0.0226
B_3-11/9	0.0225	B_3-12/8	0.0235
C_3-11/9	0.0230	C_3-12/8	0.0218
S-11/9 [10]	0.0873	FB-12/8 [32]	0.0871
FB-11/9 [46]	0.0482	FB-12/8 [47]	1.9799

The minimum time for computing optimal filters is marked in bold.

7. Generate the optimal filters using the parametric expression of the filters for the free parameter values corresponding to the minimum value of the objective function. Construct discrete-time wavelet bases from the optimal filters.
8. Repeat steps 1–7 for all the three optimization cases.

Having obtained optimal FBs, their performance has been evaluated in image compression application. Standard 8 bits per pixel (bpp) grayscale images like Lena, fingerprint [38], as well as sketch [39], straw [40], and images of various shapes [6] are used for the evaluation. For the image compression and performance analysis, we have used the following strategy: (i) Symmetrically extend the image, and apply four level discrete wavelet transform (DWT). (ii) Encode the DWT coefficients of the symmetrically extended image using set partitioning in hierarchical trees (SPIHT) [41] for a range of bit rate: 0.1–1 bpp. Decode the encoded coefficients and apply four level inverse DWT to reconstruct the image. Calculate peak signal to noise ratio (PSNR) which serves as an objective measure for the performance evaluation. Also, calculate structural similarity index (SSIM) [42] for the image reconstructed at bit rate 1 bpp. The SSIM indicates the perceptual quality of reconstructed images.

Notably, the proposed method is general in the sense that any number of iterations can be applied. We have chosen four levels of iterations for illustration. The optimal choice of the number of levels depends on the application at hand and the signal under consideration. Chang and Kuo [43] found that for the images such as Lena and some textured images, 4-level wavelet decomposition is appropriate. The authors conjectured that for the texture analysis, full decomposition of images is unnecessary and is computationally expensive. Further, in many practical applications, including the analysis of biomedical signals like an electroencephalogram (EEG), four levels of iterations have been found optimal [44,45]. Thus we apply four levels of iterations, even though the proposed method being general.

7. Results and discussions

In this section, we present certain design examples to demonstrate the effectiveness of the proposed parametrization technique and optimization method. It is followed by the performance evaluation of the designed FBs in image compression application.

We design FBs with one, two and three free parameters for the case corresponding to m=5 as discussed in Section 4. The parameters are then optimized to obtain JTFL minimized FBs. We apply four levels of iterations on the designed optimal FB which yields the discrete wavelet basis comprising five basis vectors (iterated filters). We compare the time–frequency performance of the obtained optimal FBs against equivalent CDF FBs [19] and equivalent time–frequency localized FBs designed by Sharma et al. [10].

To demonstrate the time–frequency localization properties of wavelet bases designed using the proposed technique, we minimize aforementioned objective functions for the following FBs: 11/9 FBs with three and two free parameters and 12/8 FBs with three and two free parameters. The following nomenclature is used for our JTFL optimal FBs:

$$\{\text{filter type}\}_{\{\#\text{ of free parameters}\}} - \{\text{length of analysis LPF}\}/\{\text{length of synthesis LPF}\}$$

where the filter-type can be either A or B or C corresponding to the optimality criterion, Δ_ψ or $\Delta_{\bar{\psi}}$ or $\Delta_{\psi+\bar{\psi}}$, respectively. The subscript # of free parameters denote the number of freedoms available for the optimization. For instance, the notation A_3-11/9 indicates a FB having analysis and synthesis filters of lengths 11 and 9, respectively. The filters have three free parameters, which are optimized to obtain the minimum value of the TFP of the analysis wavelet basis, Δ_ψ. We have obtained the following optimal odd-length FBs: A_2-11/9, B_2-11/9, C_2-11/9, A_3-11/9, B_3-11/9, and C_3-11/9. Similarly, we obtained the following even-length FBs: A_2-12/8, B_2-12/8, C_2-12/8, A_3-12/8, B_3-12/8, and C_3-12/8.

7.1. Time–frequency performance

Tables 3 and 4 show the time–frequency localization properties of the analysis and synthesis discrete wavelet bases along with the values of free parameters corresponding to the respective optimal FBs. In the tables, we also mention TFPs of the wavelet bases of equivalent biorthogonal CDF FB [19] and equivalent time–frequency localized S-11/9 [10] FB. For a particular number of free parameters, an optimal FB generated via optimization of a particular objective function has the least value for the respective optimality criterion compared to the other FBs in the set. Thus for odd-length FBs, A_3-11/9 has the minimum TFP, Δ_ψ for the analysis wavelet basis, B_3-11/9 has the least TFP value, $\Delta_{\bar{\psi}}$ for the synthesis wavelet basis and C_3-11/9 has the least TFP value, $\Delta_{\psi+\bar{\psi}}$ for the combination of the analysis and synthesis wavelet bases. From Table 3, it is clear that the analysis wavelet bases of the FBs A_3-11/9 and A_2-11/9 have better JTFL than the analysis wavelet bases of CDF-11/9 as well as S-11/9 FB. Similarly, the synthesis wavelet bases of the FBs, B_3-11/9 and B_2-11/9 are better JTFL than the synthesis wavelet bases of CDF-11/9 as well as S-11/9 FB. Further, the joint (average) TFP of the analysis and synthesis bases of the FBs C_3-11/9 and C_2-11/9 is lesser than that of CDF-11/9 and S-11/9 FB. It can also be observed that, with the increase in the number of free parameters, the TFPs of our design examples become lesser. Similarly for the even-length case, A_3-12/8 has the least Δ_ψ, B_3-12/8 has the least $\Delta_{\bar{\psi}}$, and C_3-12/8 has the least $\Delta_{\psi+\bar{\psi}}$. Further, from Table 4, it is evident that CDF-12/8 FB has higher TFP values compared to our even-length FBs. Fig. 4 shows frequency responses of the optimal FBs, C_3-11/9, C_3-12/8 and CDF-11/9 FB. Figs. 5 and 6 depict all basis sequences (iterated filters) of wavelet basis sequences analysis and synthesis wavelet bases corresponding to the optimal FBs C_3-11/9 and C_3-12/8 obtained by us. The TFP of each basis sequence has been mentioned in the top left hand corner of the respective figure window.

The amount of time taken by a design method to yield optimal filter coefficients is also an important consideration. To get an estimate of the time complexity of the proposed method to obtain optimal FBs and to compare it with the other optimal FB design methods [10,32,46,47], we measure the time taken by different methods to generate optimal filter coefficients (Table 5). We compare our optimal FBs with other optimal FBs, which are obtained by employing four different direct time-domain design approaches given by Sharma et al. [10,32], Patil et al. [46], and Horng and Wilson [47]. A workstation having Intel 2 GHz CORE i3 processor is used to measure the computation times. From Table 5, it is clear that the optimal FBs designed by us take lesser computation time to generate all filter coefficients compared to other optimal FBs [10,32,46,47]. Our odd-length optimal FB A_2-11/9 takes the minimum time of 0.0204 s to generate all 20 filter coefficients. The optimal FB-12/8 designed by Horng and Wilson [47] takes the highest computation time of 1.9799 s to obtain the filter coefficients.

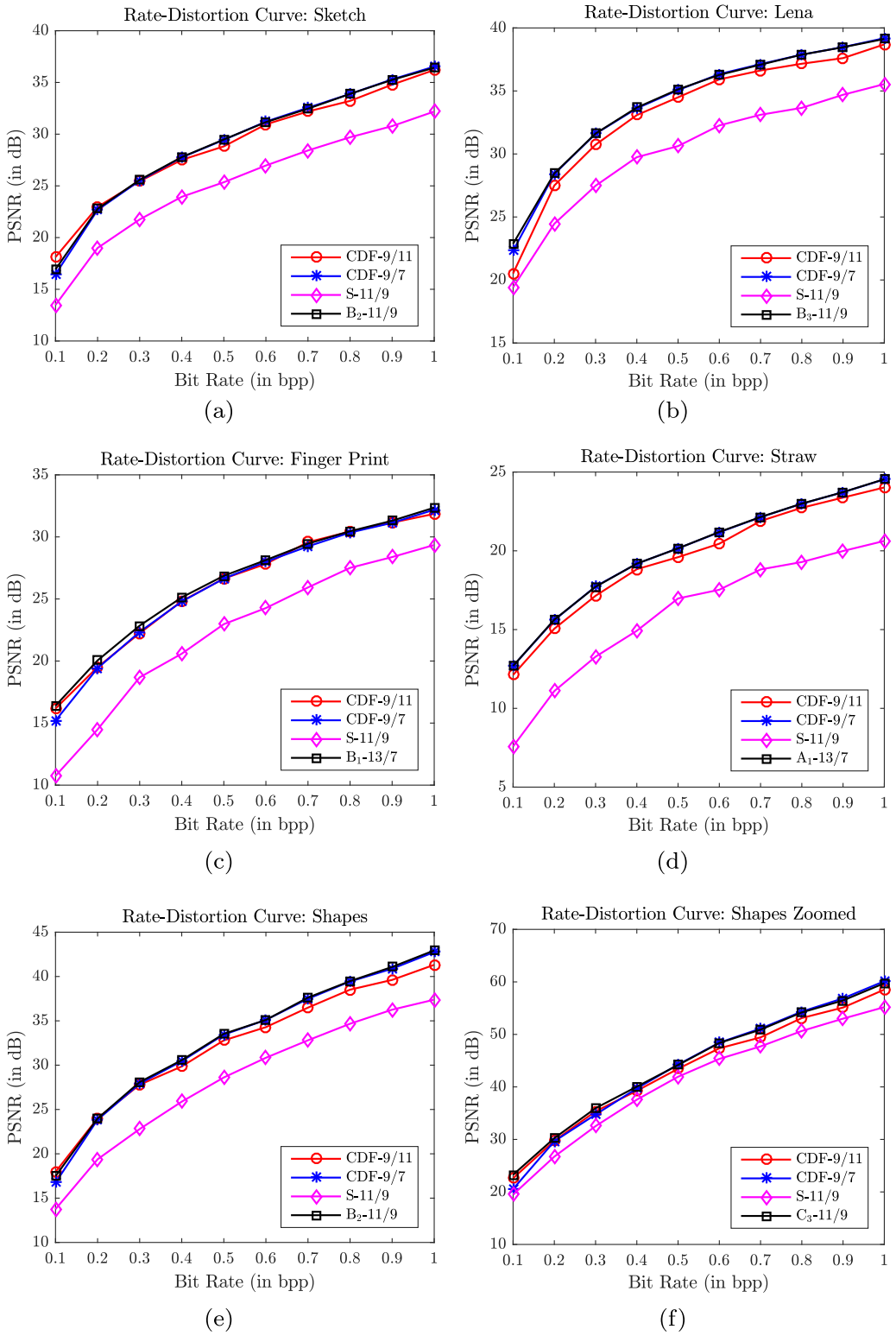

Fig. 7. Image compression performance: rate distortion plots.

Hence, the parametric design technique leads to the faster implementation of the optimal FBs. This is because, in the proposed parametric design technique, the optimal ALF and SLF are obtained simultaneously. In the complementary techniques [10,32,46,47], first one finds optimal ALF, followed by the design of optimal SLF. Hence, these techniques are two-step techniques. Whereas the optimal design employing the parametric approach is one- step technique wherein both ALF and SLF are obtained simultaneously. Moreover, irrespective of filter lengths, the number of optimization parameters is fixed in the parametrization technique. The optimization parameters are free variables which are chosen a priori to the design of FBs. The number of free variables remains lesser than the lengths of filters because of PR and VM constraints imposed on the FB. On the other hand, in the case of direct time-domain optimal design techniques [10,32,46,47] the optimal filter coefficients are obtained directly. The optimization variables are the filter coefficients. Hence, in these direct design

Table 6
Image compression performance: SSIM at bit rate 1 bpp.

FB	Image					
	Sketch	Lena	Finger print	Straw	Shapes	Shapes zoomed
CDF-11/9	0.969	0.9375	0.9686	0.9386	0.9747	0.9992
CDF-9/7	0.9737	0.9426	0.9711	0.9418	0.9823	**0.9995**
S-11/9	0.957	0.9073	0.9561	0.8625	0.9696	0.9987
A_1-13/7	0.9737	0.9427	0.971	**0.9419**	0.9822	**0.9995**
B_1-13/7	0.9731	0.9419	**0.9713**	0.941	0.9812	0.9994
C_1-13/7	0.9737	0.9426	0.9711	**0.9419**	0.9823	**0.9995**
A_2-11/9	0.9662	0.9324	0.9614	0.9297	0.9716	0.9992
B_2-11/9	**0.9746**	0.943	0.9713	0.9354	**0.9837**	**0.9995**
C_2-11/9	0.9705	0.94	0.9677	0.9386	0.9789	0.9993
A_3-11/9	0.9589	0.9196	0.9394	0.9006	0.976	0.9992
B_3-11/9	0.9737	**0.9428**	0.972	0.9377	0.9818	0.9994
C_3-11/9	0.9695	0.9393	0.9674	0.9389	0.9773	0.9994

The highest SSIM value for each image is marked in bold.

techniques, the time taken by the optimization algorithms to obtain optimal filter coefficients increases with the lengths of filters. It leads to the lesser execution time for the design of optimal filters using the proposed parametric approach. CDF [19] FBs do not provide any freedom for the optimization and are therefore not included in the comparison.

7.2. Image compression performance and comparison

For evaluating the performance of the JTFL optimized FBs in image compression application, we have used the following optimal FBs designed by us: A_3-11/9, B_3-11/9, C_3-11/9 with three parameters; A_2-11/9, B_2-11/9, C_2-11/9 with two free parameters and A_1-13/7, B_1-13/7, C_1-13/7 with one free parameter. The SPIHT algorithm has been applied on various test images at different bit rates. The rate distortion analysis has been performed in PSNR (in dB) for bit rates that range from 0.1 to 1 bpp. Fig. 7 compares the performance of our best performing FB, for the respective image, against CDF-11/9, CDF-9/7 and time–frequency localized S-11/9 FB designed by Sharma et al. [10]. Table 6 contains the structural similarity index evaluated at the bit rate of 1 bpp for the optimal FBs designed by us as well as CDF-11/9, S-11/9 and CDF-9/7.

Though, we have not found an optimal FB that globally outperforms all other FBs for all images, for every test images, one of our optimal FBs performs better compared to CDF-11/9, CDF-9/7, and previously designed time–frequency localized FBs [10]. From the rate-distortion performance plots as shown in Fig. 7(a)–(f), it is evident that for every given image, it is always possible to find an optimal FB designed by us, which has a superior rate-distortion performance than the CDF as well as previously designed time–frequency localized FBs. In particular, the optimal FB B_2-11/9 outperforms all other FBs for test image sketch. It gives an average gain of 4 dB in PSNR over S-11/9. It outperforms CDF-11/9 by an average PSNR of 0.15 dB. For Lena image, B_3-11/9 has the best performance. It gives average PSNR gains of 0.83 dB and 3.96 dB over CDF-11/9 and S-11/9, respectively. Similarly, we get B_1-13/7, A_1-13/7, B_2-11/9, and C_3-11/9 FBs as the best performing FBs for finger-print, straw, shapes, and shapes-zoomed images, respectively. The above optimal FBs give the following PSNR gains over S-11/9 FB for the respective test image: 4.01 dB, 4.01 dB, 4.75 dB, and 3.31 dB, respectively. These optimal FBs outperform CDF-11/9 FB by 0.28 dB, 0.48 dB, 0.73 dB, and 0.93 dB, for the respective images. For finger-print, shapes, and shapes-zoomed images, the performance of our optimal FBs is significantly better than the CDF-9/7 (used in JPEG-2000 image compression standard), with average PSNR gains of 0.10 dB, 0.18 dB, and 0.35 dB, respectively. In the sketch, Lena, and straw images, our FBs show competitive performance against CDF-9/7 FB, with slightly better PSNR. These optimal FBs outperform CDF-9/7 FB for the above test images by 0.04 dB, 0.06 dB, and 0.01 dB. The image quality of reconstructed images perceived by human visual systems need not necessarily be well correlated with their rate-distortion performance. Therefore, we have also calculated SSIM, which serves as a perceptual measure [42] at the bit rate 1 bpp, for all images. As per Table 6, for the sketch, Lena, fingerprint, straw and shapes, the optimal FBs; B_2-11/9, B_3-11/9, B_1-13/7, A_1-13/7 and B_2-11/9 have the highest values of SSIM, respectively. For the image zoomed-shape the SSIM corresponding to both CDF-9/7 FB and our optimal C_1-13/7 FB is the same with highest value. Thus in case of SSIM also, our optimal FBs outperform equivalent CDF and time–frequency localized FBs [10].

Though, SSIM is an indicator of perceptual measure, only visual inspection can be used to evaluate certain features of reconstructed images such as texture and edges. Fig. 8(a)–(d) compare the perceptual quality of reconstructed images at bit rate of 0.3 bpp. The images reconstructed using the FBs CDF-11/9, S-11/9, and our best performing optimal FB for the respective image are compared. The original image is shown in each figure as a reference. When the reconstructed images are zoomed for close examination, it is observed that CDF-11/9 FB introduces artifact in most of the images. It is visible on the face in the sketch image. Similarly for Lena, the artifacts are stronger on the face, edge of the hat and corner of the mirror. For the shapes image, the artifacts can be clearly seen at the edges for all shapes. For the shapes-zoomed image, artifacts are present at the edges of the square at the center of circle, and also close to the boundary of the circle. For most of the reconstructed images, S-11/9 FB have the strongest visible artifacts and information loss. However, for the shapes-zoomed image case, the edges of the square at center of its reconstructed image are comparatively clearer. But, strong artifacts are present outside the square boundary. In most of the cases, images reconstructed using our best design examples for the respective images have the least artifacts. Our reconstructed images have clearer edges, and also have lesser visual information loss compared to the other reconstructed images. Textures are preserved better by our best design examples compared to the other FBs.

To get an estimate of the time complexity of the proposed wavelet bases in the image compression application, we measure the time for analyzing each test image using the optimal FBs. Table 7 shows time taken for compressing each of the six test images corresponding to all the FBs considered by us. The compression time includes the time for generating wavelet coefficients of the image, the time taken by SPIHT algorithm for coding as well as decoding the coefficients, and the time for reconstructing the image from decoded wavelet coefficients.

8. Conclusions

We have proposed a general and very simple framework for parametric design of linear phase biorthogonal FBs of arbitrary lengths with the desired degrees of freedom and VMs. The proposed parametrization technique overcomes the restrictions on the filters that are imposed by the existing design techniques. The filter coefficients have been explicitly expressed using free parameters. The optimal free parameters can be searched to obtain minimum or maximum value of the desired objective function. We optimized these free parameters to obtain joint time–frequency localized discrete-time wavelet bases. The designed time–frequency optimized wavelet bases have noticeable improvement in TFP values over the bases generated using equivalent biorthogonal CDF FBs. The performance of the optimal FBs is evaluated in image compression application and compared with CDF biorthogonal FBs. The performance of the designed optimal FBs has been found better, both objectively and subjectively. Our proposed FBs outperform another class of previously designed time–frequency localized biorthogonal FBs [10] both objectively and subjectively. Thus, the time–frequency optimized biorthogonal linear phase FBs

(a) Sketch [39] images

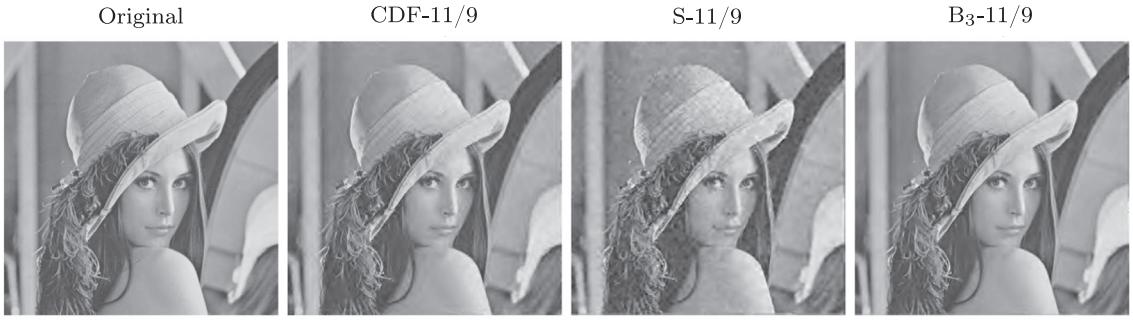

(b) Lena images

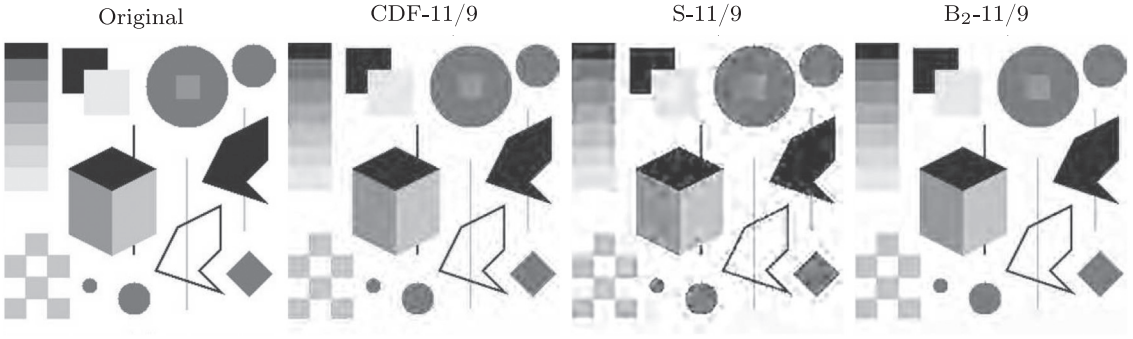

(c) Shapes [6] images

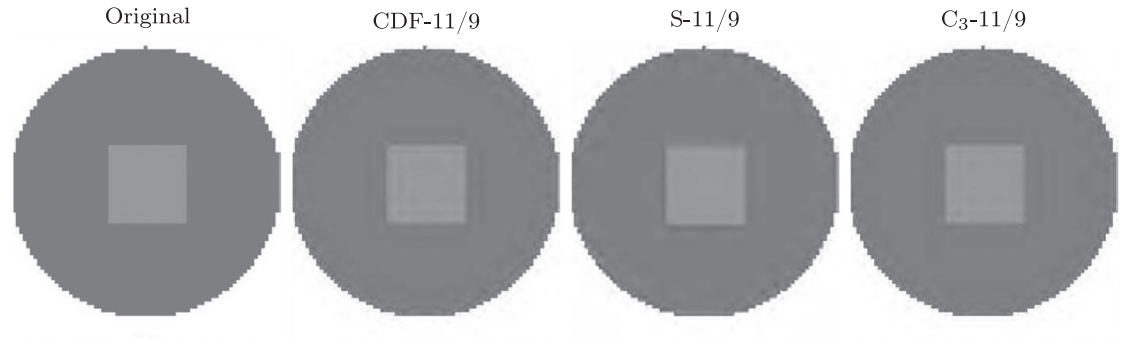

(d) Shapes-zoomed [6] images

Fig. 8. Images reconstructed, using various FBs, from level-4 DWT decomposition with bit rate 0.3 bpp.

designed by us appear promising in image compression. The proposed JTFL optimized biorthogonal wavelet bases can be regarded as a set of more compact atoms for representation of a signal in joint time–frequency domain. It is demonstrated that the proposed class of FBs perform better than the other classes of biorthogonal FBs in an image compression application. It is expected that the proposed class may perform better in some applications such as feature extraction, pulse shaping in multi-carrier communication systems, analysis and discrimination of various classes of EEG and other biomedical signals where simultaneous localization in time and frequency is essential. Performance evaluation of the time–frequency localized discrete wavelet bases in these applications would be of great interest. Further, the popular wavelet families such as CDF biorthogonal WFBs [19] and Daubechies orthogonal WFBs [17] have irrational filter coefficients. Rounding or quantization of such coefficients during hardware implementation may lead to serious problems including the

Table 7
Total time (in seconds) elapsed in wavelet decomposition, SPIHT coding as well as decoding and image reconstruction at bit rate 0.3 bpp.

FB	Image					
	Sketch	Lena	Finger print	Straw	Shapes	Shapes zoomed
CDF-11/9	27.3388	2.0731	2.5859	39.3587	2.2711	1.9242
CDF-9/7	22.7551	2.0285	2.132	44.8586	2.0916	1.7394
S-11/9	20.1229	2.0818	**1.9339**	**28.6691**	2.083	1.7265
A_1-13/7	24.0651	**2.0192**	2.1638	39.3757	2.1407	1.7748
B_1-13/7	22.4085	2.1259	2.5647	43.1094	**2.0776**	1.73
C_1-13/7	**22.2686**	2.1056	2.1446	47.4944	2.0846	1.7782
A_2-11/9	30.4894	2.122	2.5523	42.3644	2.1577	2.0108
B_2-11/9	23.2415	2.1938	2.2934	33.2056	2.1633	1.7988
C_2-11/9	23.3828	2.199	2.5524	41.4504	2.1619	1.7992
A_3-11/9	22.5304	2.1602	2.4635	43.7242	2.3217	**1.7197**
B_3-11/9	22.9789	2.1392	2.1972	31.7841	2.2079	1.7874
C_3-11/9	23.7799	2.166	2.6364	40.1441	2.2114	1.9637

The minimum of the total time for compressing each image is marked in bold.

loss of PR and VM conditions. The proposed technique which has PR and VM conditions imposed in the structure promises the design for rational filter coefficients, ensuring better hardware implementation.

References

[1] G. Strang, T. Nguyen, Wavelets and Filter Banks, Wellesley-Cambridge Press, Wellesley, Massachusetts, 1997.
[2] M. Vetterli, J. Kovacevic, V. Goyal, Foundations of Signal Processing, Cambridge University Press, Cambridge, 2014.
[3] A.K. Naik, R.S. Holambe, New approach to the design of low complexity 9/7 tap wavelet filters with maximum vanishing moments, IEEE Trans. Image Process. 23 (12) (2014) 5722–5732.
[4] M.D. Adams, D. Xu, Optimal design of high-performance separable wavelet filter banks for image coding, Signal Process. 90 (1) (2010) 180–196.
[5] T. Cooklev, A. Nishihara, M. Sablatash, Regular orthonormal and biorthogonal wavelet filters, Signal Process. 57 (2) (1997) 121–137.
[6] S. Murugesan, D.B.H. Tay, Design of almost symmetric orthogonal wavelet filter bank via direct optimization, IEEE Trans. Image Process. 21 (5) (2012) 2474–2480.
[7] D.B.H. Tay, Z. Lin, S. Murugesan, Orthogonal wavelet filters with minimum RMS bandwidth, IEEE Signal Process. Lett. 21 (7) (2014) 819–823.
[8] R. Wilson, G.H. Granlund, The uncertainty principle in image processing, IEEE Trans. Pattern Anal. Mach. Intell. PAMI-6 (6) (1984) 758–767.
[9] J.P. Gawande, A.D. Rahulkar, R.S. Holambe, A new approach to design triplet halfband filter banks based on balanced-uncertainty optimization, Digit. Signal Process. 56 (2016) 123–131.
[10] M. Sharma, V.M. Gadre, S. Porwal, An eigenfilter-based approach to the design of time–frequency localization optimized two-channel linear phase biorthogonal filter banks, Circuits Syst. Signal Process. 34 (3) (2015) 931–959.
[11] M. Sharma, D. Bhati, S. Pillai, R.B. Pachori, V.M. Gadre, Design of time–frequency localized filter banks: transforming non-convex problem into convex via semidefinite relaxation technique, Circuits Syst. Signal Process. (2016) 1–18. http://dx.doi.org/10.1007/s00034-015-0228-9.
[12] D.M. Monro, B. Bassil, G. Dickson, Orthonormal wavelets with balanced uncertainty, in: Proceedings of IEEE International Conference on Image Processing, vol. 1, IEEE, Lausanne, 1996, pp. 581–584.
[13] J.M. Morris, V. Akunuri, H. Xie, More results on orthogonal wavelets with optimum time–frequency resolution, Proc. SPIE 2491 (1995) 52–62.
[14] Y. Dandach, P. Siohan, Design method of OFDM/OQAM systems using a weighted time frequency localization criterion, in: 18th European Signal Processing Conference, IEEE, Aalborg, 2010, pp. 70–74.
[15] T. Davidson, Z.Q. Luo, K.M. Wong, Design of orthogonal pulse shapes for communications via semidefinite programming, IEEE Trans. Signal Process. 48 (5) (2000) 1433–1445.
[16] J.M. Morris, R. Peravali, Minimum-bandwidth discrete-time wavelets, Signal Process. 76 (2) (1999) 181–193.
[17] I. Daubechies, Orthonormal bases of compactly supported wavelets, Commun. Pure Appl. Math. 41 (7) (1988) 909–996.
[18] M. Vetterli, D. Le Gall, Perfect reconstruction fir filter banks: some properties and factorizations, IEEE Trans. Acoust. Speech Signal Process. 37 (7) (1989) 1057–1071.
[19] A. Cohen, I. Daubechies, J.C. Feauveau, Biorthogonal bases of compactly supported wavelets, Commun. Pure Appl. Math. 45 (5) (1992) 485–560.
[20] T. Nguyen, P. Vaidyanathan, Two-channel perfect-reconstruction FIR QMF structures which yield linear-phase analysis and synthesis filters, IEEE Trans. Acoust. Speech Signal Process. 37 (5) (1989) 676–690.
[21] P. Vaidyanathan, P. Hoang, Lattice structures for optimal design and robust implementation of two-channel perfect-reconstruction QMF banks, IEEE Trans. Acoust. Speech Signal Process. 36 (1) (1988) 81–94.
[22] I. Daubechies, W. Sweldens, Factoring wavelet transforms into lifting steps, J. Fourier Anal. Appl. 4 (3) (1998) 247–269.
[23] M. Vetterli, C. Herley, Wavelets and filter banks: theory and design, IEEE Trans. Signal Process. 40 (9) (1992) 2207–2232.
[24] D.B. Tay, Rationalizing the coefficients of popular biorthogonal wavelet filters, IEEE Trans. Circuits Syst. Video Technol. 10 (6) (2000) 998–1005.
[25] S. Murugesan, D.B.H. Tay, New techniques for rationalizing orthogonal and biorthogonal wavelet filter coefficients, IEEE Trans. Circuits Syst. I 59 (3) (2012) 628–637.
[26] R. Parhizkar, Y. Barbotin, M. Vetterli, Sequences with minimal time frequency uncertainty, Appl. Comput. Harmon. Anal. 38 (3) (2015) 452–468.
[27] E. Breitenberger, Uncertainty measures and uncertainty relations for angle observables, Found. Phys. 15 (3) (1985) 353–364.
[28] S. Starosielec, D. Hagele, Discrete-time windows with minimal RMS bandwidth for given RMS temporal width, Signal Process. 102 (2014) 240–246.
[29] M. Tazebay, A. Akansu, Progressive optimization of time–frequency localization in subband trees, in: Proceedings of the IEEE-SP International Symposium on Time–Frequency and Time-Scale Analysis, IEEE, Philadelphia, Pennsylvania, 1994, pp. 128–131.
[30] J.M. Morris, H. Xie, Minimum duration-bandwidth discrete-time wavelets, Opt. Eng. 35 (7) (1996) 2075–2078.
[31] J.M. Morris, R. Peravali, Optimum duration discrete-time wavelets, Opt. Eng. 36 (4) (1997) 1241–1248.
[32] M. Sharma, A. Dhere, R.B. Pachori, V.M. Gadre, Optimal duration-bandwidth localized antisymmetric biorthogonal wavelet filters, Signal Process 134 (2017) 87–99. http://dx.doi.org/10.1016/j.sigpro.2016.11.017.
[33] D.B. Tay, Balanced-uncertainty optimized wavelet filters with prescribed vanishing moments, Circuits Syst. Signal Process. 23 (2) (2004) 105–121.
[34] M. Sharma, R. Kolte, P. Patwardhan, V. Gadre, Time–frequency localization optimized biorthogonal wavelets, in: International Conference on Signal Processing and Communications, IEEE, Bangalore, 2010, pp. 1–5.
[35] B.D. Patil, P.G. Patwardhan, V.M. Gadre, On the design of FIR wavelet filter banks using factorization of a halfband polynomial, IEEE Signal Process. Lett. 15 (2008) 485–488.
[36] R. Ishii, K. Furukawa, The uncertainty principle in discrete signals, IEEE Trans. Circuits Syst. 33 (10) (1986) 1032–1034.
[37] R.A. Haddad, A.N. Akansu, A. Benyassine, Time–frequency localization in transforms, subbands, and wavelets: a critical review, Opt. Eng. 32 (7) (1993) 1411–1429.
[38] FVC2000 Database ⟨http://www.bias.csr.unibo.it/fvc2000/db4.asp⟩.
[39] C. Rao, G. Bhokare, U. Kumar, P. Patwardhan, V.M. Gadre, Tree structures and algorithms for hybrid transforms, in: International Conference on Signal Processing and Communications, IEEE, Bangalore, 2010, pp. 1–5.
[40] Brodatz Texture Database ⟨http://www.ux.uis.no/~tranden/brodatz/D15.gif⟩ (online; accessed 27.8.2016).
[41] A. Said, W. Pearlman, A new, fast, and efficient image codec based on set partitioning in hierarchical trees, IEEE Trans. Circuits Syst. Video Technol. 6 (3) (1996) 243–250.
[42] Z. Wang, A.C. Bovik, H.R. Sheikh, E.P. Simoncelli, Image quality assessment: from error visibility to structural similarity, IEEE Trans. Image Process. 13 (4) (2004) 600–612.
[43] T. Chang, C.C.J. Kuo, Texture analysis and classification with tree-structured wavelet transform, IEEE Trans. Image Process. 2 (4) (1993) 429–441.
[44] L. Guo, D. Rivero, J. Dorado, J.R. Rabunal, A. Pazos, Automatic epileptic seizure detection in EEGs based on line length feature and artificial neural networks, J. Neurosci. Methods 191 (1) (2010) 101–109.
[45] M. Sharma, A. Dhere, R.B. Pachori, U.R. Acharya, An automatic detection of focal EEG signals using new class of time–frequency localized orthogonal wavelet filter banks, Knowl. Based Syst., http://dx.doi.org/10.1016/j.knosys.2016.11.024.
[46] B. Patil, P. Patwardhan, V. Gadre, Eigenfilter approach to the design of one-dimensional and multidimensional two-channel linear-phase FIR perfect reconstruction filter banks, IEEE Trans. Circuits Syst. I 55 (11) (2008) 3542–3551.
[47] B.R. Horng, A.N. Willson, Lagrange multiplier approaches to the design of two-channel perfect-reconstruction linear-phase fir filter banks, IEEE Trans. Signal Process. 40 (2) (1992) 364–374.